Second Layer Nucleation in Thin Film Growth

Jörg Rottler and Philipp Maass
Fakultät für Physik, Universität Konstanz, D-78457 Konstanz, Germany
(Received 24 June 1999)

We study the second layer nucleation on top of islands emerging during epitaxial growth of thin films. By employing kinetic Monte Carlo simulations we determine the critical island radius R_c upon which small stable nuclei form in the second layer. We find that the dependence of R_c on the additional step edge barrier ΔE_s (Schwoebel barrier) is not in accordance with existing theories. Scaling arguments are presented which explain how R_c depends on ΔE_s as well as on adatom diffusion rates and on the incoming atom flux. Based on the theory, the occurrence of smooth layer-by-layer growth as opposed to rough multilayer growth is discussed.

PACS numbers: 68.55.–a, 68.35.Bs, 68.35.Fx

The onset of nucleation in the second layer of films grown by vapor deposition is of crucial importance for the resulting film structure. Smooth films growing by a layer-by-layer mode develop if stable clusters in the second layer form after coalescence of islands in the first layer, while second layer nucleation preceding island coalescence leads to a rough film morphology. As first predicted by Tersoff *et al.* [1], and later confirmed in experiment [2], the probability for second layer nucleation is connected to the existence of a critical island radius R_c: With increasing time t during evaporation, the fraction $f(t)$ of "covered islands" (i.e., on top of which a stable cluster has nucleated) rises from 0 to 1 in the vicinity of a critical time t_c; at that time the islands have acquired a mean radius R_c. Therefore, a simple criterion for the occurrence of rough multilayer growth is that R_c is smaller than the mean distance l of islands in the first layer (in the saturation regime of almost constant island density before coalescence [3]).

An important factor controlling the value of R_c is the additional step edge barrier ΔE_s [4]. This barrier has to be surmounted by an adatom, in addition to the bare surface diffusion barrier E_d, when the adatom crosses an island edge. For larger ΔE_s, one expects adatoms to remain longer on islands and therefore to accumulate more easily, which would lead to an increased second layer nucleation rate and a smaller R_c. In fact, this expectation is supported by the theory proposed in [1] that provides R_c in terms of all relevant parameters. Based on this theory, ΔE_s was estimated for various systems [2,5–8].

So far, however, the theory developed in [1] has never been tested against kinetic Monte Carlo simulations, which are an efficient tool for mimicking film growth in computer experiments [9–12] (in particular, for simulations including ΔE_s, see, e.g., Refs. [6,13]). In this Letter we report on new results of such simulations, which yield data for R_c that are in substantial disagreement with the predictions made in [1]. The discrepancy is due to the fact that in the continuum theory [1] the encounter probability for the atoms forming a stable nucleus on the island (see below) is implicitly assumed to be small, while for small critical island radii it can be on the order of one. To account for this situation we use simple scaling arguments to derive R_c. For simplicity, we restrict our analysis to the case of a critical nucleus of size $i = 1$ here, and only discuss extensions to cases with $i > 1$.

The Monte Carlo simulations were performed similiar to earlier approaches (see, e.g., [14,15]): Adatoms are deposited randomly on a triangular lattice with lattice spacing a with a rate Fa^2 per unit cell. An atom on the surface can jump to a vacant nearest neighbor site with rate $D_n/a^2 = \nu \exp[-(E_d + nE_b)/k_BT]$, where nE_b denotes the binding energy to the n in-plane nearest neighbors before the jump ($n = 0, \ldots, 5$) and k_BT is the thermal energy; ν is an attempt frequency. To account for the fast edge diffusion that leads to compact island shapes, a local relaxation mechanism is implemented, such that an atom, which finds itself in contact with at least one nearest neighbor after a jump, relaxes locally to the position with highest coordination [9]. The jump rate to cross an island edge is reduced by a factor $\alpha \equiv \exp(-\Delta E_s/k_BT)$. Simulations are performed by using a continuous time algorithm [16]. To realize a situation with $i = 1$ we have chosen $E_b/k_BT > 10$. In this case only the dimensionless parameters α and $\Gamma \equiv D_0/Fa^4$ are important.

Figure 1a shows the fraction $f(t)$ of covered islands as a function of the total coverage Fa^2t for $\alpha = 10^{-5}$ and three different Γ values. As predicted in [1], there exists a time interval, where $f(t)$ increases strongly from 0 to 1, and we define the critical time t_c for the onset of second layer nucleation by $f(t_c) = 1/2$. The mean island radius $R(t)$ [17] is shown in the inset of Fig. 1a for the same parameters. For other values of α, similiar curves are obtained. From $f(t)$ and $R(t)$ we can determine the critical radius $R_c \equiv R(t_c)$, and its dependence on α is shown in Fig. 1b for various Γ values ranging from 10^5 to 10^8 (solid symbols). Two regimes can be identified: For small $\alpha \ll \alpha_\times$ (regime I), R_c is independent of α, while for $\alpha \gg \alpha_\times$ (regime II) we find $R_c \sim \alpha^{1/7}$. The crossover value $\alpha_\times$ decreases with increasing Γ. All

 0031-9007/99/83(17)/3490(4)$15.00

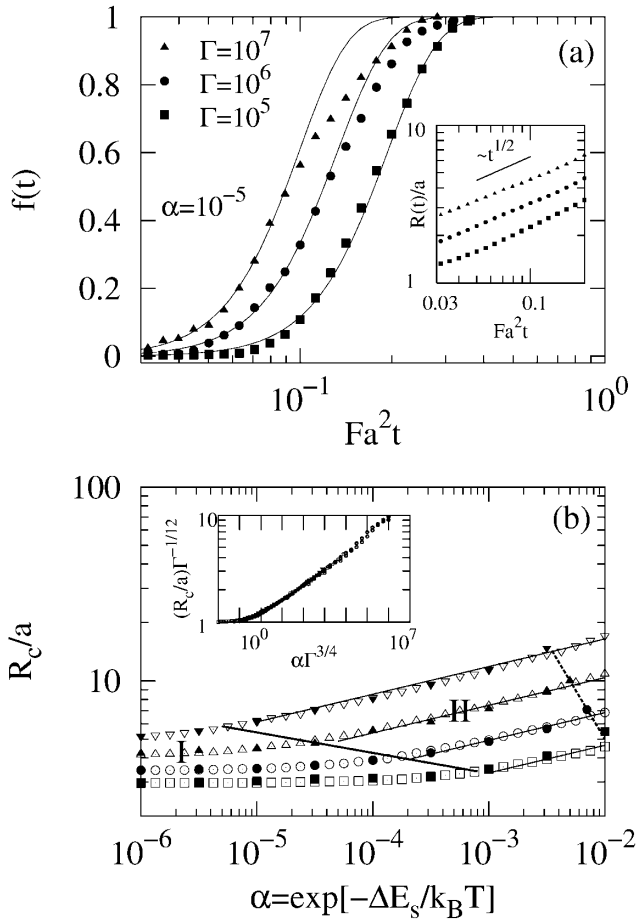

FIG. 1. (a) Three examples for the dependence of the fraction $f(t)$ of covered islands on the total coverage Fa^2t. For a given coverage, the mean radius $R(t)$ of the islands can be read off from the inset. The solid lines were calculated from the theoretical prediction for the second layer nucleation rate $\Omega[R(t)]$ (see text). (b) Dependence of the critical island radius R_c on α for four different $\Gamma = 10^5$ (■, □), 10^6 (•, ∘), 10^7 (▲, △), and 10^8 (▼, ▽). Solid symbols refer to the results from the full simulation, while open symbols refer to the results obtained from the one-island model ($R_c = 1.1R_c'$). The dashed line marks the onset of layer-by-layer growth, and the solid line with negative slope marks the border between regimes I and II; the solid lines fitting the data in regime II have slope 1/7. The inset demonstrates the scaling behavior in regimes I and II (including the data for larger Γ from Fig. 2).

curves terminate at large $\alpha \simeq \alpha_\star$ (see the disappearance of the solid symbols beyond the dashed line in Fig. 1b), when islands start to coalesce and layer-by-layer growth sets in. By contrast, from the predictions made in [1] one would expect $R_c \sim \alpha^{1/3}$ (for $\alpha \ll a/R_c$).

Next we show that the behavior of R_c can be understood by considering only one circular island, as already suggested in [1]. The radius of this island evolves in time as $R(t) = At^{1/2}$ with $A \equiv \sigma(Fa^2/\rho)^{1/2}$ in order to resemble the diffusion-mediated growth of the islands in the full simulation. Here σ is a constant independent of both α and Γ (taken from the full simulation; see the inset of Fig. 1a), and ρ is the island density, which scales as $\rho a^2 \sim \Gamma^{-1/3}$ according to standard nucleation theory [3]. This implies $A \sim F^{1/3}D_0^{1/6}$. Analogous to the full simulation, atoms are deposited onto the island and can escape from it by overcoming the additional step edge barrier. As can be seen from Fig. 1b, the critical radius R_c' obtained from this one-island model (open symbols) is the same as R_c (solid symbols) up to a constant factor, i.e., we find $R_c \cong 1.1R_c'$. (The correction factor is due to the idealized circular island perimeter in the one-island model.)

Since the computational effort is greatly reduced in the one-island model, we can obtain R_c as a function of α for an extended range of Γ values (see Fig. 2). Moreover, R_c is defined for $\alpha > \alpha_\star$, and in accordance with the predictions made in [1] there occurs a further regime IV for $\alpha \gg a/R_c$, where R_c is independent of α. Between regimes II and IV a transient regime III exists, the significance of which will be discussed below.

We now present simple scaling arguments, which can explain our results. To this end we first note that, for small α (regimes I and II), the second layer nucleation almost always takes place once two atoms are present on the island. In order to find two atoms on the island, one atom has first to be deposited and then to "survive" on the island until a second atom is deposited (see also [18]). However, if the probability p_s, for such a nucleation trial to be successful, is much smaller than one, the first atom generally leaves the island before the deposition of a second atom. To nucleate a second layer, a mean number $n \gg 1$ of trials is then necessary so that $np_s \simeq 1$.

For a given island radius R, let us consider the characteristic time $\Delta t(R)$ during which R does not change significantly. Since the island radius grows algebraically in

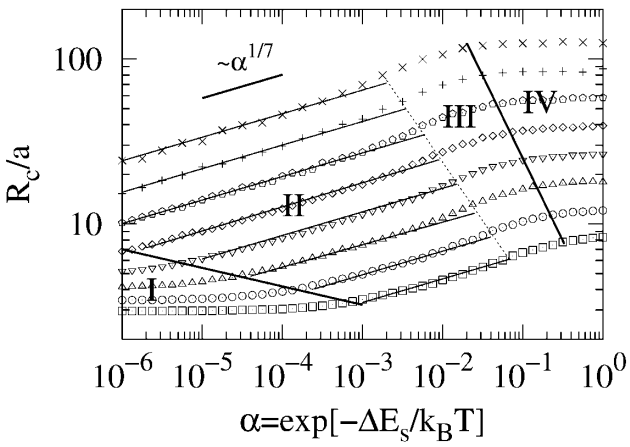

FIG. 2. Critical island size R_c as a function of α obtained from the one-island model for eight different Γ values starting from 10^5 (□) and ending at 10^{12} (×). Between these values, Γ is increased by a factor of 10. The various regimes I–IV are indicated, together with the border line with slope $(-1/9)$ between regimes I and II and the border line with slope (-1) between regimes III and IV. The dashed border line separating the transient regime III from regime II was calculated from the condition $\omega_e(R_c)t_s(R_c) \simeq 1$ (see text).

time, there is no characteristic time scale for changing $R(t)$ other than t itself; that means

$$\Delta t(R) \sim t \sim R^2/A^2 \sim R^2 F^{-2/3} D_0^{-1/3}. \quad (1)$$

[For example, changing $R(t)$ by 10% takes a time $\Delta t(R) = 0.21t = 0.21R^2/A^2$.] Within the time interval $\Delta t(R)$, the mean number of nucleation trials is $n \simeq \pi R^2 F \Delta t(R)$. The probability that an atom is deposited during the presence of another atom is $p_s \simeq 1 - \exp[-\pi F R^2 t_s(R)]$, where [19]

$$t_s(R) \simeq \frac{R}{D_0}\left(\frac{a}{\alpha} + \zeta R\right) \quad (2)$$

is the characteristic survival time on the island with radius R (ζ is a constant of order unity). Accordingly, the condition $np_s \simeq 1$ for second layer nucleation reads

$$R_c^2 F \Delta t(R_c)\{1 - \exp[-\pi R_c^2 F t_s(R_c)]\} = \text{const}. \quad (3)$$

Taking $\Delta t(R_c)$ from Eq. (1) and $t_s(R_c) \simeq R_c a/D_0\alpha$ for $\alpha \ll a/R_c$, we can deduce two limiting cases from Eq. (3): For $\pi R_c^2 F t_s(R_c) \simeq \pi R_c^3/\alpha\Gamma a^3 \gg 1$ (regime I) we find $R_c/a \sim \Gamma^{1/12}$, while for $\pi R_c^3/\alpha\Gamma a^3 \ll 1$ (regime II) we obtain $R_c/a \sim \Gamma^{4/21}\alpha^{1/7}$. Hence, we can write

$$\frac{R_c}{a} \sim \begin{cases} \Gamma^{1/12} & \text{for } \alpha \ll \alpha_\times \\ \Gamma^{4/21}\alpha^{1/7} & \text{for } \alpha \gg \alpha_\times \end{cases}, \quad (4)$$

where $\alpha_\times \sim \Gamma^{-3/4}$ [note that $R_c(\alpha_\times) \sim \alpha_\times^{-1/9}$, which implies that the boundary line between regimes I and II has slope $(-1/9)$ (see Figs. 1b and 2)]. The validity of Eq. (4) is demonstrated in the inset of Fig. 1b, which shows the collapse of data from regime I and II onto one master curve. Moreover, the result for regime I is consistent with the behavior in the limit $\alpha \to 0$, which is particularly simple. Here, the nucleation takes place directly after the deposition of the second atom ($n = 1$). The average time after the second deposition is $\tau = (5/2FA^2)^{1/2}$ in a continuum description [20]. Hence, $R_c = A\tau^{1/2} \sim (A^2/F)^{1/4} \sim \Gamma^{1/12}a$, in agreement with Eqs. (3) and (4) [the exact result for τ can be used to estimate the constant in Eq. (3)].

So far we have assumed that nucleation always takes place once two atoms are on the island. This assumption ceases to be valid for larger α in regimes III and IV of Fig. 2. In these regimes we have to take into account that two atoms may fail to encounter during the survival time $t_s(R)$. Since the mean distance of two atoms on the island is proportional to R, the characteristic rate for the encounter scales as

$$\omega_e(R) \sim D_0/R^2, \quad (5)$$

and we can estimate the encounter probability p_e to be $p_e \simeq 1 - \exp[-\omega_e(R)t_s(R)]$. However, we found the scaling law (5) to be valid only for large $R \gg 100a$. For smaller R, corrections to scaling are important. The condition $np_s p_e \simeq 1$ for second layer nucleation now reads

$$R_c^2 F \Delta t(R_c)\{1 - \exp[-\pi R_c^2 F t_s(R_c)]\} \times \{1 - \exp[-\omega_e(R_c)t_s(R_c)]\} = \text{const}, \quad (6)$$

where the last term becomes important if $\omega_e(R_c)t_s(R_c) \ll 1$.

For $\alpha \ll a/R_c$ we have $t_s(R_c) \simeq R_c a/D_0\alpha$ from Eq. (2), but when inserting the scaling law (5) into the condition $\omega_e(R_c)t_s(R_c) \ll 1$ we get $\alpha \gg a/R_c$. Nevertheless, due to the corrections to (5) for small R, both conditions $\alpha \ll a/R_c$ and $\omega_e(R_c)t_s(R_c) \ll 1$ can be fulfilled in a transient regime III. In this regime there exists no definite scaling of R_c with α and Γ, and to determine R_c one must use the function $\omega_e(R)$ and then solve the implicit condition (6) numerically. [Moreover, from the condition $\omega_e(R_c)t_s(R_c) = 1$ we have calculated the dashed border line between regimes II and III shown in Fig. 2.]

For $\alpha \gg a/R_c$, $t_s(R_c) \simeq R_c^2/D_0$ and $\omega_e(R_c)t_s(R_c)$ becomes independent of R_c, α, and Γ for large R_c (and only weakly dependent on R_c for small R_c). We thus obtain

$$R_c/a \sim \Gamma^{1/6} \text{ for } \alpha \gg a/R_c \quad (7)$$

corresponding to regime IV in Fig. 2.

Figure 3 depicts the various regions characterizing the mechanism of second layer nucleation in an $\alpha - \Gamma$ diagram. Varying Γ and α within one of the regions results in the corresponding behavior of R_c according to Eqs. (4) and (7). The border line between regions I and II has slope $(-4/3)$, between regions III and IV slope (-6), and the dashed line marks the border line between regions II and III. In addition, we have drawn the transition line from rough multilayer to smooth layer-by-layer growth into the diagram. In our simulations island coalescence occurs in regime II (see Fig. 1b), where $R_c \sim \Gamma^{4/21}\alpha^{1/7}$. The criterion $R_c \simeq l \sim \rho^{-1/2} \sim \Gamma^{1/6}$ thus yields $\alpha_\star \sim \Gamma^{-1/6}$.

Up to now we have focused on homoepitaxial film growth with a critical nucleus of size $i = 1$. It is straightforward, however, to extend the analysis to other cases. In general, $i + 1$ atoms have to be deposited and have to

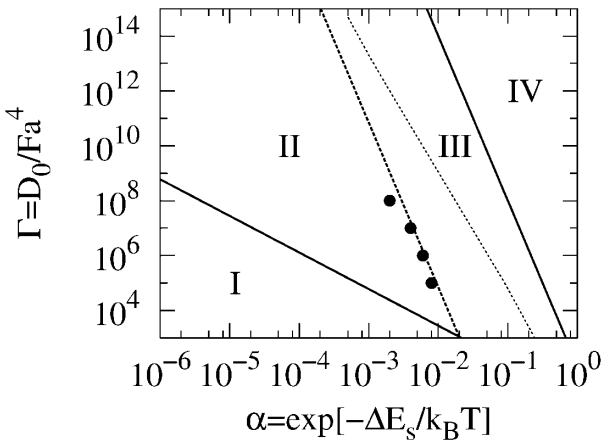

FIG. 3. The various regions characterizing the mechanism of second layer nucleation in an α-Γ diagram. The thick dashed line with slope (-6) marks the onset of layer-by-layer growth [the circles refer to the onset of island coalescence obtained in the full simulation (see Fig. 1b)].

encounter each other during the survival time $t_s(R)$. The corresponding nucleation condition reads $np_s^i p_e^{(i)} \simeq 1$, where $p_e^{(i)} \simeq 1 - \exp[-\omega_e^{(i)}(R_c)t_s(R_c)]$ is the encounter probability of $i+1$ atoms and $\omega_e^{(i)}(R) \sim (D_0/a^2)(a^2/R^2)^i$ is the encounter rate [21]. Using $\rho \sim \Gamma^{-i/(i+2)}$ [3] (i.e., $A \sim F^{1/2}\rho^{-1/2} \sim F^{1/(i+2)}D_0^{i/2(i+2)}$), we then obtain $R_c/a \sim \Gamma^\gamma \alpha^\mu$ with the following exponents: regime I $(\alpha \ll \alpha_\times)$—$\gamma = i/4(i+2)$, $\mu = 0$; regime II $(\alpha_\times \ll \alpha \ll \alpha'_\times)$—$\gamma = i(i+3)/(i+2)(3i+4)$, $\mu = i/(3i+4)$; regime III $(\alpha'_\times \ll \alpha \ll a/R_c)$—$\gamma = i(i+3)/(i+2)(i+5)$, $\mu = (i+1)/(i+5)$; regime IV $(\alpha \gg a/R_c)$—$\gamma = i/2(i+2)$, $\mu = 0$. The crossover values scale as $\alpha_\times \sim \Gamma^{-\delta}$ and $\alpha'_\times \sim \Gamma^{-\delta'}$ with $\delta = (i+8)/4(i+2)$ and $\delta' = i(i+3)(2i-1)/2(i+2)(i^2+i+2)$, respectively. We note that, for $i \geq 2$, regime III becomes a true scaling regime, which corresponds to that predicted in [1] for small $\alpha \ll a/R_c$. Hence, the results of [1] can be viewed as resulting from the scaling arguments for large R_c corresponding to $\alpha \gg \alpha'_\times$ (and $i \geq 2$).

In the case of heteroepitaxy, one has to distinguish between the adatom diffusion rate D_0/a^2 on an island and the rate D_{0s}/a^2 on the substrate surface. Since D_{0s} enters the scaling analysis only via the constant $A \sim F^{1/3}D_{0s}^{1/6}$ in the growth law $R(t) = At^{1/2}$, one can readily redo the above calculations. For example, for $i = 1$, one obtains $R_c \sim \Gamma_s^{1/12}$ for $\alpha \ll \alpha_\times$ (regime I) and $R_c \sim \Gamma^{1/7}\Gamma_s^{1/21}\alpha^{1/7}$ for $\alpha \gg \alpha_\times$ (regime II) with $\Gamma_s \equiv D_{0s}/Fa^4$ and $\alpha_\times \sim \Gamma^{-1}\Gamma_s^{1/4}$. Similiarly, other growth laws for $R(t)$ can be treated, which in experiments may be realized by special preparation techniques (see, e.g., [2]).

Finally, let us discuss our findings with respect to recent experiments tailored to extract the step edge barrier. An important ingredient in the analysis of such experiments [2,8] is the second layer nucleation rate $\Omega(R)$. In our approach, $\Omega(R)$ is given by the mean number np_sp_e of sucessful nucleation trials in time $\Delta t(R)$ divided by $\Delta t(R)$, i.e., $\Omega(R) = \pi R^2 F\{1 - \exp[-\pi R^2 F t_s(R)]\}\{1 - \exp[-\omega_e(R)t_s(R)]\}$. With $\Omega(R)$ specified, the distribution $f(t)$ can be calculated as in [1] through $f(t) = 1 - \exp\{-\int_0^t dt'\,\Omega[R(t')]\}$ as long as the island size distribution $\chi(R,t)$ is sufficiently sharply peaked at about $R(t)$. The solid lines in Fig. 1a were determined in this way and give an excellent fit to the simulated data for $f(t) \lesssim 0.5$. When $f(t)$ approaches one, deviations occur, which become more pronounced with increasing Γ. The deviations are caused by the broadening of $\chi(R,t)$ with t [10]: The small islands with radii much smaller than $R(t)$ are covered at later times than islands with radii comparable to $R(t)$. We suggest that the experimental data for estimating ΔE_s be reanalyzed in light of the results presented here.

We are indebted to R. J. Behm, W. Dieterich, and H. Wedler for very helpful discussions. P. M. thanks the Deutsche Forschungsgemeinschaft (SFB 513, Ma 1636/2-1) for financial support.

[1] J. Tersoff, A. W. Denier van der Gon, and R. M. Tromp, Phys. Rev. Lett. **72**, 266 (1994).
[2] K. Bromann, H. Brune, H. Röder, and K. Kern, Phys. Rev. Lett. **75**, 677 (1995).
[3] J. A. Venables, G. D. T. Spiller, and M. Hanbücken, Rep. Prog. Phys. **47**, 399 (1984).
[4] G. Ehrlich and F. G. Hudda, J. Chem. Phys. **44**, 1039 (1966); R. L. Schwoebel, J. Appl. Phys. **40**, 614 (1969).
[5] J. A. Meyer, J. Vrijmoeth, H. A. van der Vegt, E. Vlieg, and R. J. Behm, Phys. Rev. B **51**, R14 790 (1995).
[6] P. Šmilauer and S. Harris, Phys. Rev. B **51**, R14 798 (1995).
[7] I. Markov, Phys. Rev. B **54**, 17 930 (1996).
[8] K. R. Roos and M. C. Tringides, Surf. Rev. Lett. **5**, 833 (1998).
[9] M. C. Bartelt and J. W. Evans, Surf. Sci. **423**, 189 (1999); M. C. Bartelt and J. W. Evans, Surf. Sci. Lett. **314**, L829 (1994).
[10] J. G. Amar and F. Family, Thin Solid Films **272**, 208 (1996); J. G. Amar, F. Family, and P.-M. Lam, Phys. Rev. B **50**, 8781 (1994).
[11] M. Bott, M. Hohage, M. Morgenstern, T. Michely, and G. Comsa, Phys. Rev. Lett. **76**, 1304 (1996); S. Liu, Z. Zhang, G. Comsa, and H. Metiu, Phys. Rev. Lett. **71**, 2967 (1993).
[12] H. Brune, Surf. Sci. Rep. **31**, 121 (1998).
[13] C.-M. Zhang, M. C. Bartelt, J.-M. Wen, C. J. Evans, and P. A. Thiel, J. Cryst. Growth **174**, 851 (1997).
[14] C. Ratsch, A. Zangwill, P. Šmilauer, and D. D. Vvedensky, Phys. Rev. Lett. **72**, 3194 (1994).
[15] G. S. Bales and D. C. Chrzan, Phys. Rev. B **50**, 6057 (1994).
[16] K. Binder and D. W. Heermann, *Monte Carlo Simulations in Statistical Physics*, Springer Series in Solid State Science Vol. 80, (Springer, Berlin, 1992), 2nd ed.
[17] The radius R of an island is defined as $R = (s/\pi)^{1/2}a$, where s is the number of atoms of the island.
[18] Z. Zhang and M. G. Lagally, Phys. Rev. Lett. **72**, 693 (1994); Z. Zhang and M. G. Lagally, Science **276**, 377 (1997).
[19] A simple explanation for this result is that for large α the survival time is given by the characteristic time $t \sim R^2/D_0$ for an atom to reach the boundary, while for small α an atom typically returns many times to the boundary before escaping from the island. In the latter limit, the characteristic escape rate (inverse survival time t_s^{-1}) can be estimated to be the product of the probability $2\pi Ra/\pi R^2$ for the atom to be at the boundary and the rate $\alpha D_0/a^2$ to overcome the step edge barrier.
[20] The time-dependent deposition rate $W(t)$ onto the circular island is given by $W(t) = \pi R^2(t)F$ when neglecting lattice effects (continuum description). Accordingly, $\phi(t_2,t_1) = \exp[-\int_{t_1}^{t_2} dt\,W(t)]$ is the probability that no atom is deposited between times t_1 and $t_2 > t_1$. The probability $\psi(t_2,t_1)dt_2dt_1$ that the first and second atom are deposited in time intervals $(t_1, t_1 + dt_1)$ and $(t_2, t_2 + dt_2)$ is $\psi(t_2,t_1) = W(t_2)\phi(t_2,t_1)W(t_1)\phi(t_1,0)$, from which τ follows after averaging.
[21] This holds true for an idealized situation, where the lifetimes of intermediate subcritical clusters can be neglected.